Coumarin sulfonamides derivatives as potent and selective COX-2 inhibitors with efficacy in suppressing cancer proliferation and metastasis

Xiao-Yuan Lu, Zhong-Chang Wang, Shen-Zhen Ren, Fa-Qian Shen, Ruo-Jun Man, Hai-Liang Zhu

PII: S0960-894X(16)30648-5
DOI: http://dx.doi.org/10.1016/j.bmcl.2016.06.037
Reference: BMCL 23990

To appear in: *Bioorganic & Medicinal Chemistry Letters*

Received Date: 20 April 2016
Revised Date: 12 June 2016
Accepted Date: 15 June 2016

Please cite this article as: Lu, X-Y., Wang, Z-C., Ren, S-Z., Shen, F-Q., Man, R-J., Zhu, H-L., Coumarin sulfonamides derivatives as potent and selective COX-2 inhibitors with efficacy in suppressing cancer proliferation and metastasis, *Bioorganic & Medicinal Chemistry Letters* (2016), doi: http://dx.doi.org/10.1016/j.bmcl.2016.06.037

Coumarin sulfonamides derivatives as potent and selective COX-2 inhibitors with efficacy in suppressing cancer proliferation and metastasis

Xiao-Yuan Lu†, Zhong-Chang Wang†*, Shen-Zhen Ren, Fa-Qian Shen, Ruo-Jun Man, Hai-Liang Zhu*

State Key Laboratory of Pharmaceutical Biotechnology, Nanjing University, Nanjing 210023, People's Republic of China

*Corresponding author. Tel. & fax: +86-25-89682572; e-mail: zhuhl@nju.edu.cn,
†These two authors equally contributed to this paper.

Abstract

Cyclooxygenase-2 is frequently overexpression in malignant tumors and the product PGE_2 promotes cancer cell progression and metastasis. We designed novel series of coumarin sulfonamides derivatives to improve biological activities of COX-2 inhibition and anticancer. Among them, compound **7t** showed most powerful selective inhibitory and antiproliferative activity (IC_{50} = 0.09 μM for COX-2, IC_{50} = 48.20 μM for COX-1, IC_{50} = 0.36 μM against HeLa cells), comparable to the control positive compound **Celecoxib** (0.31 μM, 43.37 μM, 7.79 μM). Cancer cell apoptosis assay were performed and results indicated that compound **7t** effectively fuels HeLa cells apoptosis in a dose and time-dependent manner. Moreover, **7t** could significantly suppress cancer cell adhesion, migration and invasion which were essential process of cancer metastasis. Docking simulations results was further indicated that compound **7t** could bind well to the COX-2 active site and guided a reasonable design of selective COX-2 inhibitor with anticancer activities in future.

Keywords:

Coumarin

Sulfonamides

COX-2 inhibitor

Anticancer

Docking simulation

Inflammation had emerged as a dominating factor promoting cancer progression. [1, 2] Inflammatory mediators including cytokines, chemokines, and growth factors promoted cancer cell growth. [3, 4] Prostaglandin E_2 which acted as inflammatory mediators influence many mechanisms that played a significant role in tumorigenesis such as cell proliferation, angiogenesis, apoptosis, and metastasis. [5, 6] Prostaglandins including PGE_2 were derived from arachidonic acid catalyzed by two isoforms cyclooxygenase: the constitutive COX-1 and the inducible COX-2. [7] COX-1 protein was ubiquitously expressed a wide range of tissues, whereas COX-2 was an inducible enzyme that could promptly up-regulated by mediator of triggering inflammation and thus was in the charge of acute increases in PGs synthesis. [8, 9] COX-2 overexpression was a characteristic feature of most malignant tumor and contributed to poor outcomes in multiple malignancies.[10-12]

Recent studies have demonstrated that COXs inhibitor **Aspirin** combined with immunotherapies promoted much more rapid tumor regression and eradication of cancer cells than immunotherapies alone. [4] These researches caused mechanisms of cyclooxygenase-dependent tumor and COXs inhibitors have been taken seriously. COXs inhibitors have been therapy in many clinical diseases including atherosclerosis, endothelial dysfunction, neuroinflammation, preterm labor, Parkinson's disease, and cancer.[13-15] In fact, the interruption of COX-1, particularly in the gastrointestinal system, may lead to dangerous side effects such as ulcers. [16] COX-2-dependent PGE_2 biosynthesis has been identified promoting cell progression, metastasis and survival in a variety of tumors. [17-19] COX-2 selective inhibitors necessarily represent a potentially useful class of anticancer drugs, such as **Celecoxib** have been shown to decrease mammary and colorectal tumor burden in animal models by increasing tumor cell apoptosis, decreasing proliferation, and suppressing metastasis. [10, 20]

Most of selective COX-2 inhibitors were characterized by diarylheterocycle often substituting SO_2NH_2 or SO_2Me moiety at *para*-position of one of the aryl rings, such as **Celecoxib (1)**, **SC-558 (2)**, **Valdecoxib** (**3**), **Etoricoxib** (**4**). COX-2 selective

inhibition potency of these coxibs were verified by multiple researches and docking simulations. [21-23] **Celecoxib** exhibited most potent chemopreventive activity in these COX-2 inhibitors. It owned 1,5-diarylpyrazole structure containing sulfanilamide group and should be an ideal lead COX-2 inhibitors with potent anticancer activity. [24, 25]

Based on the structure of **Celecoxib**, 1,5-diarylpyrazole class of analogs were designed and synthesized in this study. 4-chlorocoumarin and acylhydrazones moieties were selected as pharmacophore to explore more powerful and high-efficiency COX-2 inhibitor with anticancer activities. Coumarins were chosen due to their derivatives are extensively found in different natural products and possessed compelling wide-ranging biological activities, such as antibacterial, antioxidant, anti-inflammatory and anticancer. [26-28] Coumarin derivatives were linked by introduction of acylhydrazones group which has been widely used in the design of new bioactive compounds with prominent pharmacological profiles. [29]

On the basis of this finding, we designed 20 novel acylhydrazone and 4 -chlorocoumarin-substituted 1,5-diarylpyrazoles benzenesulfonamide derivatives (**7a-7t**) to explore efficacy in COX-2 inhibition and cancer suppression. **7t** was found and showed significant selective COX-2 inhibition as effective anticancer drugs which could accelerate cancer cells apoptosis, inhibit proliferation, migration and invasion.

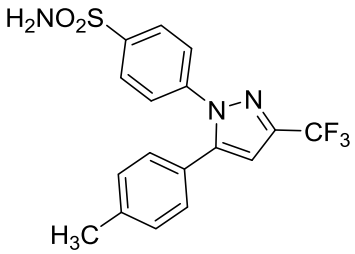

Celecoxib (1)

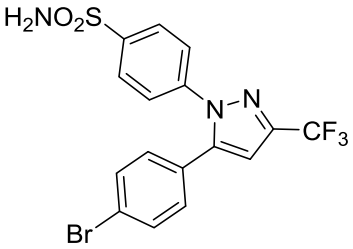

SC-558 (2)

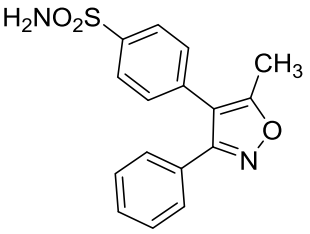

Valdecoxib (3)

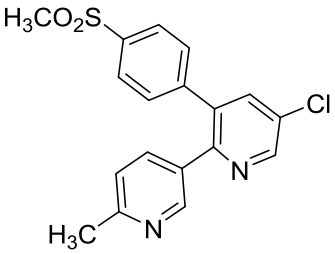

Etoricoxib (4)

Figure 1. Selective COX-2 inhibitors

The routes to synthesis the acylhydrazone and 4-chlorocoumarin-substituted 1,5-diarylpyrazoles benzenesulfonamide derivatives according to the general pathway outlined in **Scheme 1**. And the structures of the target compounds are shown in **Table 1**. The various substituted chalcones (**2a-2t**) were carried out using dimethyl oxalate and the substituted acetophenone under vigorous stirring with excessive sodium methoxide in refluxing methanol. Then **(3a-3t)** was prepared according to the reaction of different chalcones with 4-hydrazinylbenzenesulfonamide in methanol. Compounds **3a-3t** was added a solution of hydrazine monohydrate and ethanol under vigorously stirred at 80 °C from several hours to overnight to obtain compounds **4a-4t**. 4-hydroxycoumarin was transformed to 4-chloro-coumarin- 3-aldehyde in mixture of phosphoric trichloride and dimethyl formamide. Finally, compounds **4a-4t** were converted into the corresponding target compounds **7a-7t** by reacting with 4-chloro-coumarin-3-aldehyde (**6**) in 60 % ~90 % yield. All the compounds are reported for the first time. All of the target compounds gave satisfactory analytical and spectroscopic data ^{1}H NMR, ^{13}C NMR, EI-MS, which are in accordance with their depicted structures.

Scheme 1[a].

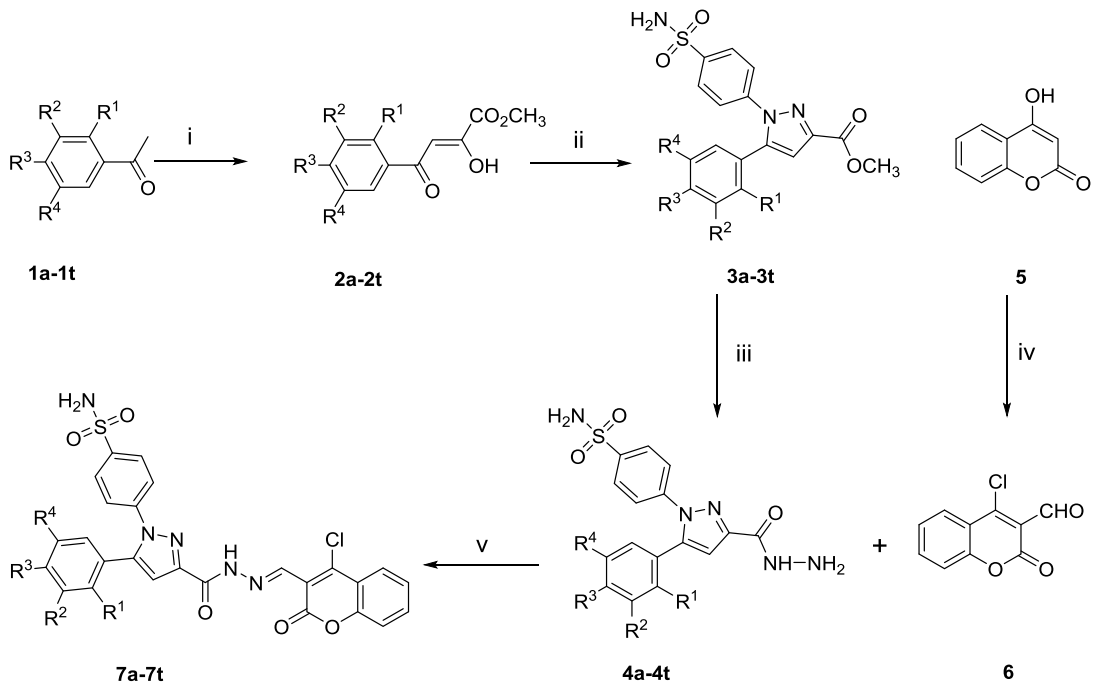

[a] General synthesis of compounds (**7a-7t**). Reagents and conditions: (i) 2.0 equiv dimethyl oxalate, MeOH, MeONa, reflux, 6 h; (ii) 1.0 equiv 4-hydrazinyl benzenesulfonamide, MeOH, reflux, 6 h; (iii) 10.0 equiv hydrazine hydrate, EtOH, reflux, 8 h; (iv) $POCl_3$, DMF, 0 °C to rt, 2h, then 60 °C, 6h; (v) EtOH, AcOH, rt, 12 h.

Table 1. Chemical structure of compounds **7a-7t**.

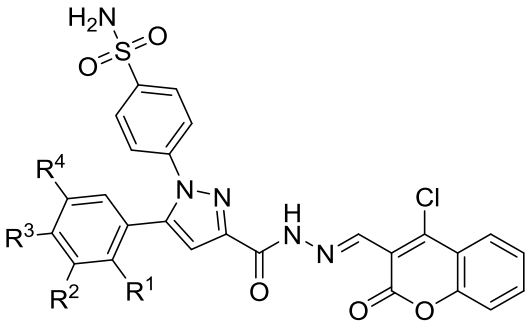

Compounds	R^1	R^2	R^3	R^4
7a	H	H	H	H
7b	H	H	CH_3	H
7c	H	CH_3	H	H
7d	CH_3	H	CH_3	H
7e	H	CH_3	CH_3	H
7f	H	H	OCH_3	H

7g	H	OCH_3	H	H
7h	H	OCH_3	OCH_3	H
7i	H	OCH_3	OCH_3	OCH_3
7j	H	H	OCH_2CH_3	H
7k	OH	H	H	H
7l	H	H	OH	H
7m	Cl	H	H	H
7n	H	Cl	H	H
7o	H	Cl	Cl	H
7p	F	H	H	H
7q	H	F	H	H
7r	H	H	F	H
7s	H	H	NO_2	H
7t	H	H	CF_3	H

All synthesized derivatives (**7a-7t)** were evaluated for their *in vitro* antiproliferation activities against four cancer cell lines (HeLa, HepG2, F10, A549) and two non-cancer cell lines (293T, L02) with the positive control drugs **Celecoxib**. The outcomes were summarized up in **Table 2.** The results indicated that most of the target compounds can powerfully inhibit the proliferation of the HeLa and HepG2 cells. The IC_{50} values of compounds **7a-7t** against HeLa cell lines were between 0.36 and 16.19 μM and HepG2 cell lines were range from 0.85 to 21.19 μM. Furthermore, all compounds had lower toxicity against the non-cancer cells 293T and L02 than **Celecoxib** with these compounds minimum IC_{50} of 293T and L02 cells were 101.24 μM and 104.57 μM. Among them, compound **7t** displayed the most potent anti-tumor activity in HeLa with IC_{50} of 0.36 μM, compared to the positive control Celecoxib (IC_{50} =7.79 μM). Moreover, **7t** possess weak toxicity toward 293T and L02 cells with IC_{50} of 293T and L02 cells were 234.46 μM and 267.28 μM, compared to the toxicity of **Celecoxib (**95.26, 98.15 μM**)**. Thus it can be seen that introduction of acylhydrazone and chlorocoumarin moieties obviously promoted the activities of antiproliferation and attenuated toxicity activities, the results demonstrated the two moieties in synthesized compounds were significant for anticancer activities.

Table 2. Inhibition of cell proliferation against HeLa, HepG2, F10, A549, 293T, L02 cells by target compounds (**7a-7t**)

Compounds	IC_{50}[a] (μM)					
	HeLa[b]	HepG2[b]	F10[b]	A549[b]	293T[b]	L02[b]
7a	9.86±0.76	5.76±0.42	9.53±0.65	33.52±1.64	179.99±4.57	182.52±4.64
7b	8.81±0.73	11.27±1.21	6.22±0.53	22.14±1.21	188.63±5.21	>300
7c	11.08±0.86	5.98±0.51	5.28±0.48	20.26±0.98	>300	199.27±4.82
7d	7.95±0.51	6.70±0.57	4.68±0.34	28.46±1.32	175.00±4.67	206.23±4.96
7e	6.92±0.54	4.41±0.45	6.93±0.72	24.23±1.41	232.64±5.39	>300
7f	12.02±1.02	14.68±1.26	7.31±0.84	31.48±1.82	>300	>300
7g	7.58±0.63	15.66±1.34	9.58±0.87	22.41±1.07	106.62±2.43	104.57±2.73
7h	13.12±1.12	21.19±1.41	19.80±1.36	40.14±1.76	174.96±3.68	187.14±3.92
7i	16.19±1.26	20.04±1.29	26.24±1.57	26.14±1.13	101.24±2.27	116.35±2.69
7j	8.76±0.82	17.03±1.08	10.33±1.05	24.34±1.09	105.46±2.76	112.25±2.85
7k	11.67±0.98	19.94±1.24	20.92±1.49	17.16±0.97	>300	159.26±3.43
7l	12.43±1.14	18.23±1.05	21.32±1.61	26.42±1.57	138.52±3.08	163.34±3.68
7m	5.09±0.35	6.10±0.40	9.12±0.86	12.28±1.03	253.72±5.04	214.09±4.65
7n	5.46±0.39	6.75±0.51	15.62±1.17	14.66±1.10	151.54±3.26	168.32±3.89
7o	4.91±0.51	5.12±0.36	7.45±0.61	23.46±1.17	153.07±3.59	>300
7p	2.85±0.27	5.94±0.39	6.41±0.52	14.34±1.08	107.68±2.39	147.75±3.76
7q	3.43±0.42	4.74±0.24	8.79±0.85	16.17±1.22	155.06±4.07	205.87±5.26
7r	0.94±0.12	3.53±0.16	9.76±1.02	11.24±0.87	181.36±4.63	192.27±5.03
7s	0.52±0.09	1.63±0.12	4.04±0.31	3.85±0.42	112.87±2.84	133.41±3.34
7t	0.36±0.05	0.85±0.08	2.27±0.17	2.56±0.34	234.46±4.52	267.28±4.87
Celecoxib	7.79±0.84	10.03±0.84	14.36±0.96	15.64±1.23	95.26±2.28	98.15±2.39

[a] Antiproliferation activity and cytotoxicity was measured using the MTT assay. Data shown are the mean ±SD of three independent experiments (n=3) run in triplicate.

[b] Cancer and non-cancer cells kindly supplied by State Key Laboratory of Pharmaceutical Biotechnology, Nanjing University.

Compounds **7a-7t** was evaluated for their ability to inhibit COX-1 and COX-2 using human COX-1/COX-2 ELISA Kit and results were showed in **Table 3** indicated that the majority of the synthesized compounds exhibited excellent selectivity inhibiting COX-2 activities displaying IC_{50} values between 0.09 and 21.93 μM. Among them, **7t** was the most active and significant selectivity with IC_{50} value of inhibition COX-2/ COX-1 were 0.09, 48.20 μM, which owned better cyclooxygenase selective inhibition capability with the positive control drug **Celecoxib** with IC_{50}

value of 0.31 μM, 43.37 μM.

The subsequent structure-activity relationship (SAR) studies were performed to determine how the substituents affect the COX-2 inhibitory activities. We found change of substituents -R^3 (*para*-position) could greatly affect the activities of COX-2 inhibition. When substituents -R^1, -R^2, -R^4 kept immutability, the changes with different substituents -R^3 for COX-2 inhibition activity showed electron-withdrawing groups on *para*-position are preferable than electron-donating groups. For instance, the active gradients for compounds were **7t** (0.09 μM), **7s** (0.13 μM) >**7r** (0.17 μM)> **7a** (4.53 μM), **7b** (6.94 μM)> **7j** (8.83 μM), **7l** (9.97 μM), **7f** (10.36 μM). The inhibitory activities increased in the following order: CF_3, NO_2 >F >H, CH_3> OCH_3, OCH_2CH_3, OH. While -R^2 or -R^1 were modified, the inhibition activity result indicated that electron-withdrawing groups performed better than electron-donating groups in the same way. As shown in inhibition of COX-2: **7q** (0.26 μM) >**7n** (0.54 μM) > **7a** (4.53 μM), **7c** (4.79 μM), **7g** (6.09 μM); **7p** (0.47 μM)> **7m** (1.06 μM)> **7a** (4.53 μM), **7k** (7.57 μM).

From the above mentioned analysis, it could be concluded that change for substituent -R^3 caused remarkable variation of inhibitory activity, with the substituent -R^3 (such as CF_3, NO_2), exhibited more potent COX-2 inhibition and anticancer activities than those have electron-donating substituents (such as OCH_3, CH_3, OH). This promising finding would provide a direction to design and optimize more effective COX-2 inhibitors with anticancer activity.

Table 3. Inhibition activities of compounds (**7a-7t**) against COX-1/COX-2

Compounds	IC_{50}, μM^a		COX-1/COX-2 ratio
	COX-1	COX-2	
7a	>100	4.53±0.53	>22
7b	89.53±2.06	6.94±0.72	12.9
7c	48.21±1.42	4.79±0.60	10.0
7d	39.45±1.33	7.13±0.81	5.5
7e	>100	6.25±0.66	>16
7f	84.27±2.21	10.36±0.94	8.1
7g	>100	6.09±0.75	>16
7h	69.25±1.83	10.41±0.79	6.6

7i	49.76±1.52	21.93±1.26	2.7
7j	78.54±2.10	8.83±0.83	8.89
7k	>100	7.57±0.67	>13
7l	>100	9.97±1.23	>10
7m	86.24±2.47	1.06±0.21	81.35
7n	>100	0.54±0.15	>185
7o	96.59±2.61	0.30±0.09	322.9
7p	>100	0.47±0.13	>212
7q	74.30±1.96	0.26±0.10	285.7
7r	53.43±1.74	0.17±0.06	314.3
7s	42.16±1.25	0.13±0.04	324.1
7t	48.20±1.30	0.09±0.01	>500
Celecoxib	43.37±1.44	0.31±0.12	139.9

[a]COX-1/COX-2 inhibitory activity was measured using the human COX-1/COX-2 assay kit. Values shown are the mean ±SD of three independent experiments (n=3) run in triplicate.

Subsequently, we investigated the effect of compound **7t** on HeLa cell apoptosis. We treated HeLa cells with different concentrations (1, 2, 4, 8 μM) of compound **7t** for 24 h and treated with 3 μM **7t** for different times (0, 12, 24, 36 h) and analyzed cells for changes in apoptotic markers with a flow cytometer *in vitro*, as shown in **Figure 2**, the percentage of apoptosis cell were 4.1%, 5.7%, 13.9%, 35.8%, 49.2%, corresponding to the concentration of 0, 1, 2, 4, 8 μM, that revealed apoptosis cells significantly increased after treatment with high doses of compound **7t**. Meanwhile, **7t** also causing cell apoptosis in a time-dependent manner that the percentage of apoptosis cell were 3.8%, 6.8%, 23.6%, 31.8% when treated with 3 μM for 0, 12, 24, 36 h. From the above, **7t** could effectively causing HeLa cell apoptosis in a dose and time-dependent manner.

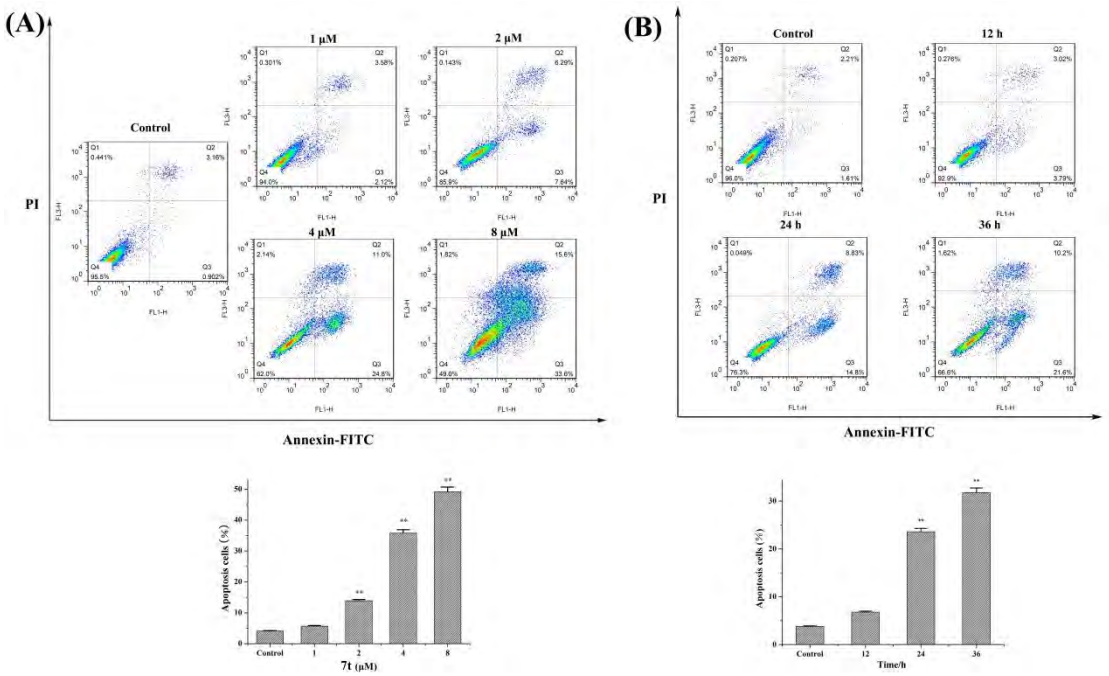

Figure 2. Annexin V-FITC/PI dual-immuno-fluorescence staining after treatment with different concentrations of **7t** for different times revealed significantly increased number of apoptotic cells. (A) Compound **7t** induced apoptosis in HeLa cells with the density of 0, 1, 2, 4, 8 μM for 24 h were collected and processed for analysis. (B) Cells treated with 3 μM **7t** for different times (0, 12, 24, and 36 h) was collected and analyzed. The percentage of cells in each part was indicated. Images are representative of three independent experiments. Data are mean ±S.E.M. of three independent experiments (n=3). $^{*}P < 0.05$, $^{**}P < 0.01$.

Cell adhesion plays a significant role in cancer progression and metastasis. Herein, we investigated the adhesive ability of HeLa cells as affected by **7t** and positive control drug **Celecoxib**. HeLa cells (2×10^5 per well) were treated with different doses of **7t** and **Celecoxib** for the adhesion assay to detect their inhibition of adhesive ability. The data shown in **Figure 3** indicated that **7t** could effectively reduce the attachment of HeLa cells but the effects of **Celecoxib** were not obvious in low dose. Indeed, at low dose of 2 μM **7t**, the attachment decreased about 60%.

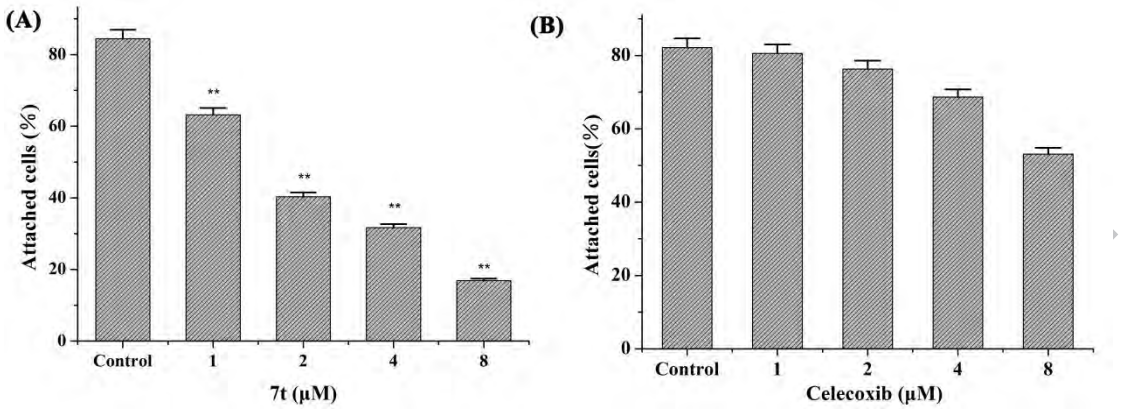

Figure 3. Compound **7t** caused dose-dependent decrease of HeLa cell attachment. (A) Influence of **7t** on HeLa cell adhesion. (B) Influence of **Celecoxib** on HeLa cell adhesion. Data shown are the mean ±S.E.M. of three independent experiments (n=3). $^{*}P < 0.05$, $^{**}P < 0.01$.

Metastasis is multistage process that results from the convergence of a variety of cellular processes. Some of these processes include cell migration, invasion, adhesion into the surrounding stroma and through vessel walls, and survival in a foreign environment. Cancer cell migration and invasion are the initial steps in metastasis. So we investigated the effect of **7t** on migration and invasion of HeLa cell using 8 μm 24-well transwell. As shown in **Figure 4**, a significant decrease in cell migration was observed with increased concentration of **7t**, compared with control. Furthermore, we conducted transwell invasion assays to evaluate the potency of **7t** on cancer cell invasion. The results showed that HeLa cancer cells significantly lost their ability to invade through the matrigel matrix and the number of cells that invaded through the matrigel matrix was observably decreased. These data suggest that **7t** could effectively suppress cancer cell migration and invasion.

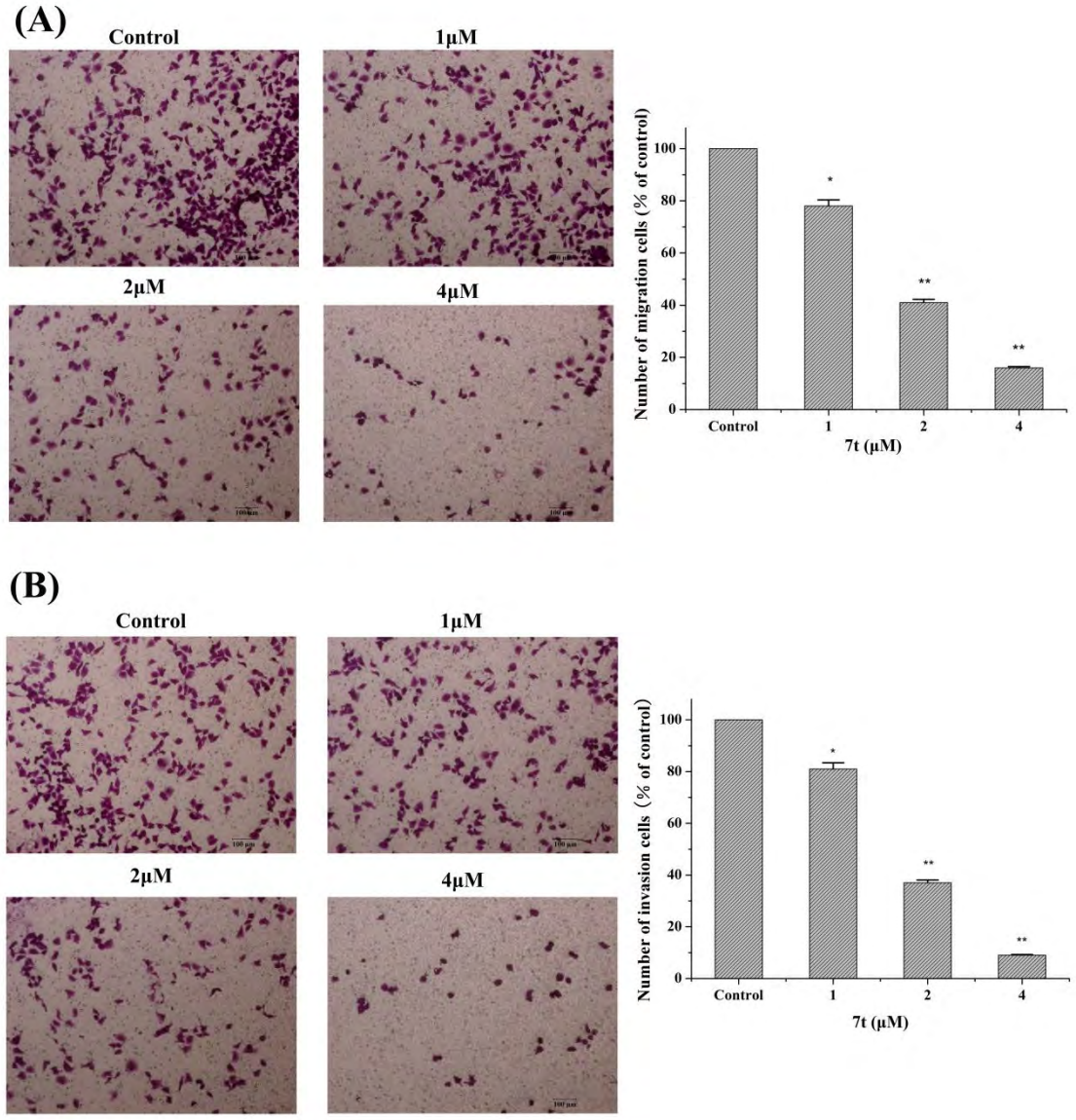

Figure 4. Compound **7t** significantly inhibits HeLa cells migration and invasion. (A) The images (×100) of cells that migrated outside of transwell insert membrane in transwell migration assay. (B) The images (×100) of cells that invaded through the matrigel to outside of transwell insert membrane in transwell invasion assay. The number of migrated and invaded cells was counted in 16 random fields per chamber of three independent experiments (n=3). $^{*}P < 0.05$, $^{**}P < 0.01$.

We determined the secretion of PGE_2 in HeLa cells after treatment with LPS, **Celecoxib** and **7t** for 24 h. The result shown in **Figure 5** indicated that **7t** significantly reduced synthesis and secretion of PGE_2 in HeLa cells. Compared to **Celecoxib,** the effect of **7t** on PGE_2 secretion was more pronounced. In order to verify whether **7t** effects on anticancer were mediated by COX-2/PGE_2 pathway, we investigated the effects of PGE_2, COX-2 inhibitor **7t** and **7t**+PGE_2 on cellular proliferation, adhesion,

apoptosis, migration, and invasion under identical experimental conditions in HeLa cells using method described previously with some modifications. As shown in **Figure 6A**, PGE_2 promoted proliferation of HeLa cells in a certain extent. **7t** was able to completely reverse PGE_2 induced cancer cell proliferation. Likewise, PGE2 caused cancer cell adhesion and apoptosis could be inverted by **7t** (**Figure 6B and 6C**). Based on these encouraging results, we subsequently determined whether PGE_2 could increase migration and invasion of cancer cell *in vitro* and **7t** could s uppress this tendency caused by PGE_2. Fortunately, migration and invasion of HeLa cells was reasonably stimulated by PGE_2, **7t** was capable of reversing PGE_2 induced cancer cell migration and invasion. These data suggested that PGE_2 indeed mediate proliferation, adhesion, apoptosis, migration, and invasion of HeLa cells. **7t** participated in the COX-2/PGE_2 pathway acted as COX-2 inhibitor and thus exert efficacy in suppressing cancer proliferation and metastasis.

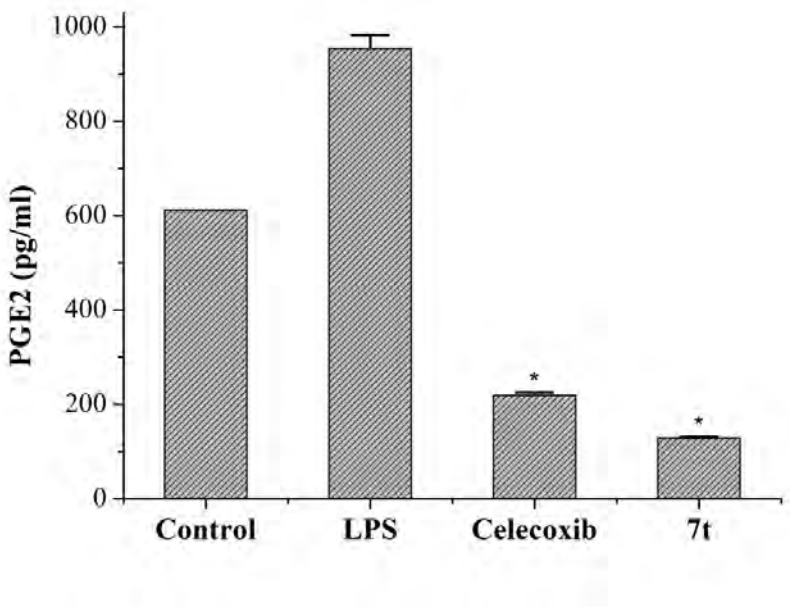

Figure 5. The effects of **7t** (0.1 μM), **Celecoxib** (0.1 μM), LPS (0.1 μg/ml) on PGE_2 secretion in HeLa cells. Data shown are the mean ±S.E.M. of three independent experiments (n=3). $^{*}P < 0.05$.

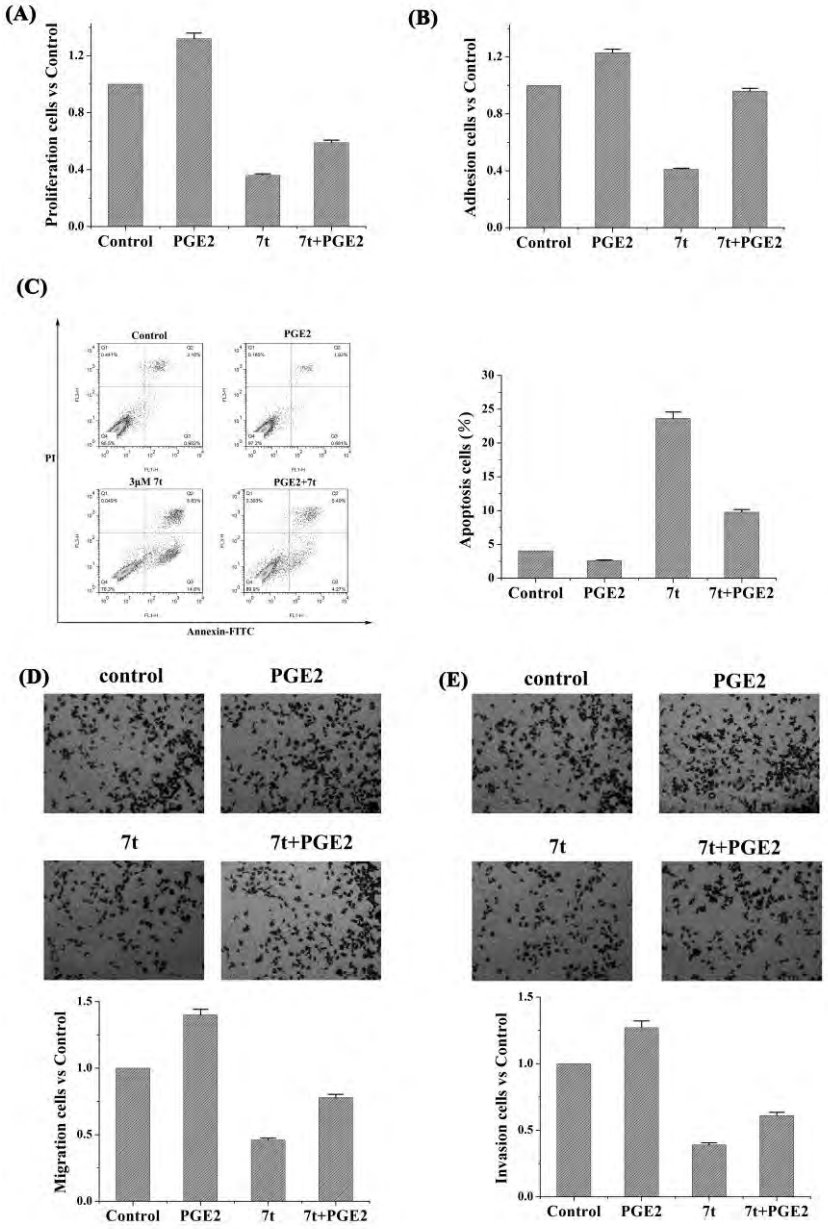

Figure 6. The effects of PGE_2 (1 μM), **7t** (2μM) and **7t** (2 μM)+PGE_2 (1 μM) on HeLa cell proliferation, adhesion, apoptosis, migration, and invasion. (A) The effects of PGE2, **7t** and **7t**+PGE2 on cell proliferation were determined using MTT assay. (B) The effects of PGE_2, **7t** and **7t** +PGE_2 on cell adhesion. (C) The effects of PGE_2, **7t** (3 μM) and **7t** (3 μM) +PGE_2 on cell apoptosis. (D) The effects of PGE_2, **7t** and **7t** +PGE_2 on cell migration. (E) The effects of PGE_2, **7t** and **7t** +PGE_2 on cell invasion. Data shown are the mean ±S.E.M. of three independent experiments.

Docking study was performed to gain a better understand the potency of compound **7t** and further guide structure-activity relationship (SAR) research, we proceeded to examine the interaction of **7t** and **Celecoxib** with COX-2 (PDB code:

3PGH). All amino acid residues of COX-2 that interacted with compound **48** and **Celecoxib** were exhibited in pictures **Figure 7**, **Figure 8** and **Figure 9**. The estimated interaction energies of synthesized compounds were ranging from -46.85 to -66.41 kcal/mol, as displayed in **Figure 7** and **Figure 8.** In the binding mode, **Celecoxib** binds to COX-2 with binding free energy were -49.72 kcal/mol via two hydrogen bonds with **TRP387**, two Pi bonds and a Sigma-Pi bond with **HIS207**. However, compound **7t** had a best estimated binding free energy of -66.41 kcal/mol and bound superiorly to COX-2 through four hydrogen bonds, two Pi bonds and a Sigma-Pi bond. As shown in **Figure 8**, three amino acids, **GLN203**, **HIS207**, **ASN382** significantly bound with **7t**. The **GLN203**, **HIS207, ASN382** formed four hydrogen bonds with **7t** (angle O · H-N = 161.98°, distance = 1.96 Å, angle O · H-N = 140.07°, distance = 1.98 Å, angle H · O-C = 145.75°, distance = 2.23 Å, angle H · N-N = 136.30°, distance = 2.36 Å). Furthermore, compound **7t** was also bonded with **His207** by two Pi bonds (distance = 3.59 Å, distance = 3.94 Å) and a Sigma-Pi bond (distance = 2.70 Å). The results indicated that acylhydrazone, benzenesulfonamide, pyrazole ring, chlorocoumarin moieties are crucial for activities of compound and these with biological assay data suggested that **7t** could be a potential inhibitor of the COX-2.

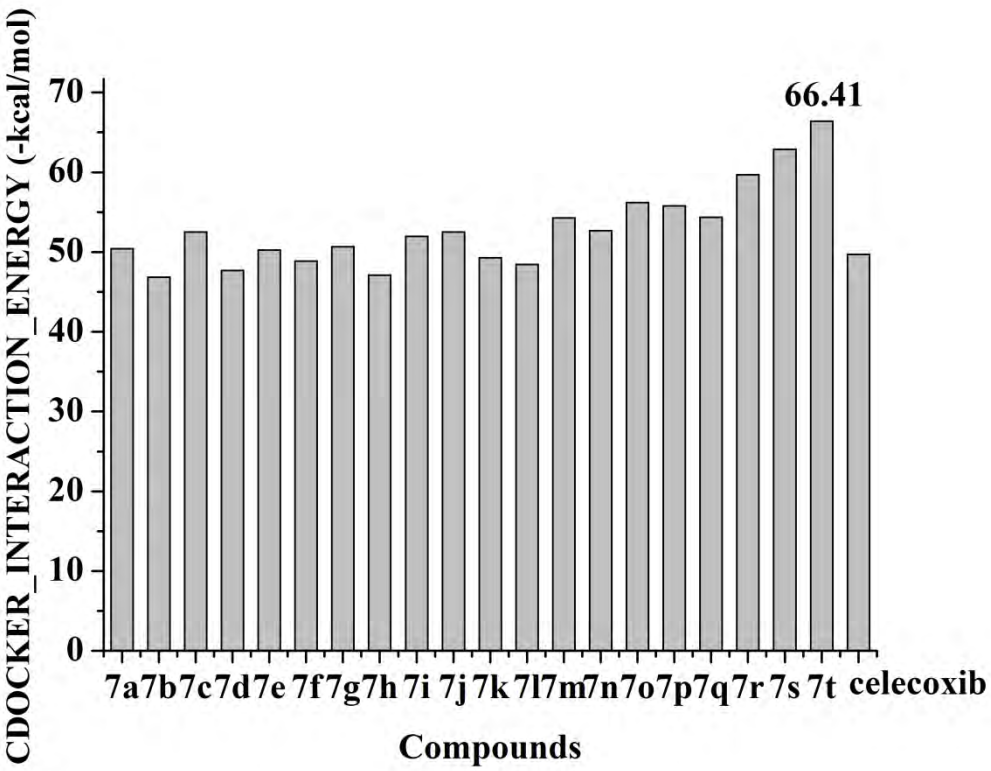

Figure 7. The histogram about CDOCKER_INTERACTION_ENERGY (-kcal/mol) of compounds (**7a-7t**) and **Celecoxib** for COX-2.

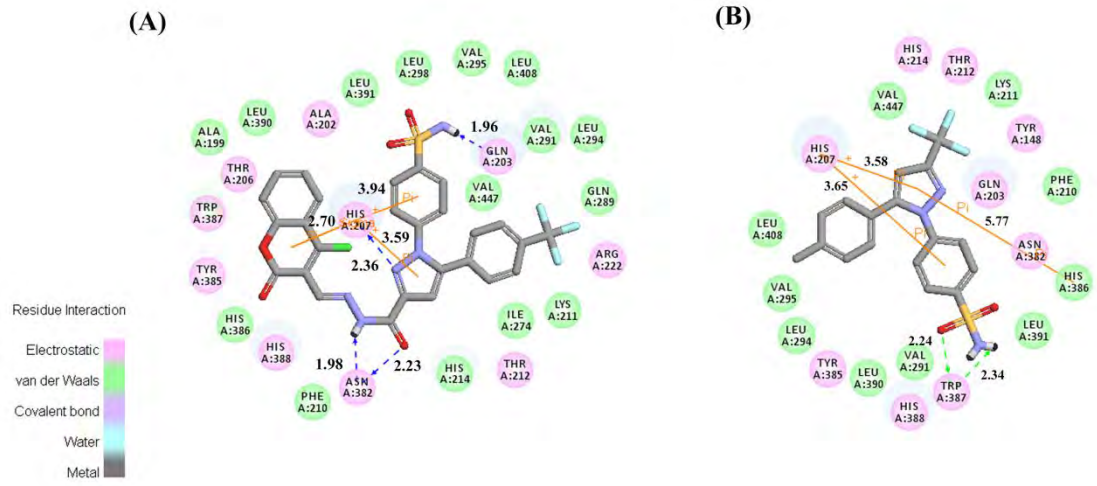

Figure 8. Molecular docking analysis of compound **7t** and **Celecoxib**, showing **7t** owned remarkable binding mode in COX-2. (A) Molecular docking 2D modeling of compound **7t** with COX-2: for clarity, only interacting residues are displayed. Three amino acids, **GLN203**, **HIS207**, **ASN382** was significant in the binding of ligand and formed four hydrogen bonds, two Pi bonds and a Sigma-Pi bond (B) Molecular docking 2D modeling of **Celecoxib** with COX-2: Three

amino acids **HIS207, HIS386, TRP387** in enzyme formed two Pi bonds, a Sigma-Pi bonds and two hydrogen bonds with **Celecoxib**.

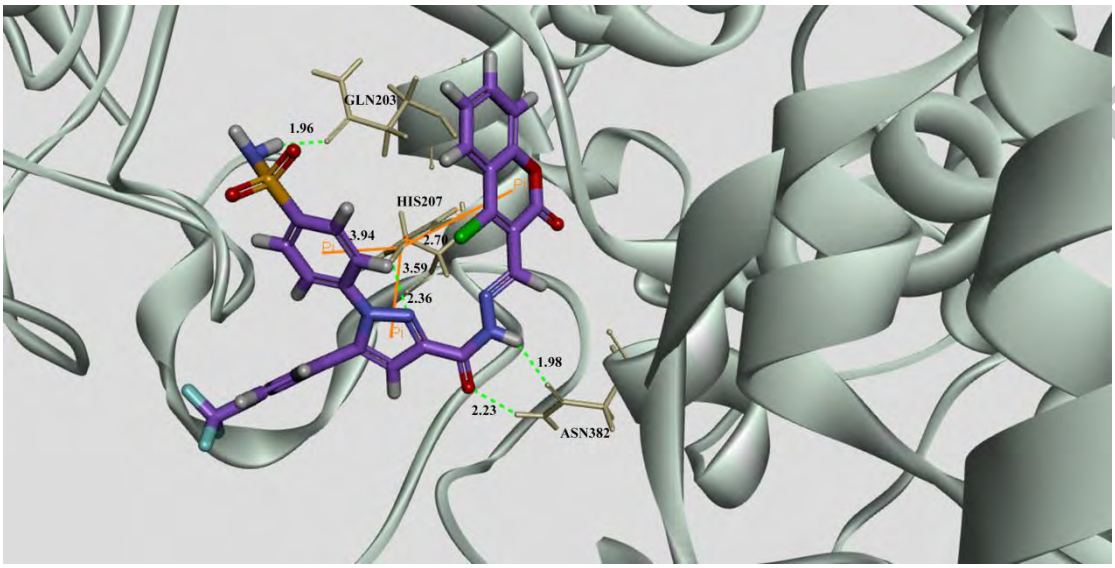

Figure 9. Molecular docking 3D modeling of compound **7t** with the COX-2 binding site: for clarity, only interacting residues are displayed.

In summary, the tumorigenic effects and metastatic potential of COX-2 in the tissue are largely determined to be attributed to its role in producing PGE_2. It is worth noting that COX-2/PGE_2 pathway inhibition was useful in the prevention of malignant tumors. In our study, a series of novel COX-2 inhibitors possess extraordinarily potent antiproliferative activities against HeLa, HepG2, A549, F10 cells and COX-2 selectivity inhibition activities. Among these compounds, compound **7t** showed the most powerful antiproliferative activity (IC_{50} = 0.36 μM for HeLa cells) and COX-2 inhibitory activity (IC_{50} =0.09 μM). In addition, **7t** can induce cancer cell apoptosis in a dose and time-dependent manner. Inhibition of cancer cell adhesion, migration and invasion which were pivotal processes in cancer progression and metastasis were also detected and results indicated that **7t** possess high-efficiency performance on characteristic feature of malignant tumor. We investigated the effects of PGE_2, **7t** and **7t**+PGE_2 *in vitro* cellular experiment to verify PGE_2 involved in proliferation and metastasis of HeLa cells and **7t** could completely reverse PGE_2 induced progression of cancer cell by operating in COX-2/PGE_2 pathway.

The probable binding mode proposed by the docking simulation might be a

convincing explanation of the impressive performance of compound **7t**, in which **7t** binds eminently to COX-2 through four hydrogen bonds, two Pi bonds and a Sigma-Pi bond with best estimated binding free energy of -66.41 kcal/mol. **Celecoxib** binds to COX-2 was less stable than that of **7t** and possess undesirable anticancer activities. This result indicated acylhydrazone, chlorocoumarin and electron-withdrawing moieties are crucial for anticancer activities of synthesized derivatives. It can be concluded that compound **7t** as well as the other coumarin sulfonamides derivatives are promising leads for further study as potential anticancer COX-2 inhibitor.

Acknowledgement

The work was financed by a grant (No.J1103512) from National Natural Science Foundation of China and the Fundamental Research Funds for the Central Universities (No.020814380011) and the Projects (Nos.CXY1409 & CG1305) from the Science & Technology Burea of Lianyungang City of Jiangsu Province.

References and notes

1. Coussens, L. M.; Zitvogel, L.; Palucka, A. K. *Science* **2013,** *339*, 286.
2. Mantovani, A.; Allavena, P.; Sica, A.; Balkwill, F. *Nature* **2008,** *454*, 436.
3. Balkwill, F.; Charles, K. A.; Mantovani, A. *Cancer Cell* **2005,** *7*, 211.
4. Zelenay, S.; van der Veen, A. G.; Böttcher, J. P.; Snelgrove, K. J.; Rogers, N.; Acton, S. E.; Chakravarty, P.; Girotti, M. R.; Marais, R.; Quezada, S. A. *Cell* **2015,** *162*, 1257.
5. Konturek, P.; Kania, J.; Burnat, G.; Hahn, E.; Konturek, S. *J. Physiol. Pharmacol.* **2005,** *56*, 57.
6. Vo, B. T.; Morton Jr, D.; Komaragiri, S.; Millena, A. C.; Leath, C.; Khan, S. A. *Endocrinology* **2013,** *154*, 1768.
7. Vitale, P.; Tacconelli, S.; Perrone, M. G.; Malerba, P.; Simone, L.; Scilimati, A.; Lavecchia, A.; Dovizio, M.; Marcantoni, E.; Bruno, A. *J. Med. Chem.* **2013,** *56*, 4277.
8. Cui, P. H.; Rawling, T.; Bourget, K.; Kim, T.; Duke, C. C.; Doddareddy, M. R.; Hibbs, D. E.; Zhou, F.; Tattam, B. N.; Petrovic, N. *J. Med. Chem.* **2012,** *55*, 7163.
9. Rigas, B.; Kashfi, K. *J. Pharmacol. Exp. Ther.* **2005,** *314*, 1.
10. Ho, M.-Y.; Liang, S.-M.; Hung, S.-W.; Liang, C.-M. *Cancer Res.* **2013,** *73*, 439.
11. Limongelli, V.; Bonomi, M.; Marinelli, L.; Gervasio, F. L.; Cavalli, A.; Novellino, E.; Parrinello, M. *Proc. Nat.l Acad. Sci. U. S. A.* **2010,** *107*, 5411.
12. Suh, Y.; Afaq, F.; Johnson, J. J.; Mukhtar, H. *Carcinogenesis* **2009,** *30*, 300.
13. Biava, M.; Porretta, G. C.; Poce, G.; Supino, S.; Forli, S.; Rovini, M.; Cappelli, A.; Manetti, F.; Botta, M.; Sautebin, L. *J. Med. Chem.* **2007,** *50*, 5403.

14. G Perrone, M.; Scilimati, A.; Simone, L.; Vitale, P. *Curr. Med. Chem.* **2010,** *17*, 3769.
15. Tao, L.; Wang, S.; Zhao, Y.; Sheng, X.; Wang, A.; Zheng, S.; Lu, Y. *Phytomedicine* **2014,** *21*, 1473.
16. Pal, M.; Madan, M.; Padakanti, S.; Pattabiraman, V. R.; Kalleda, S.; Vanguri, A.; Mullangi, R.; Rao Mamidi, N. V. S.; Casturi, S. R.; Malde, A.; Gopalakrishnan, B.; Yeleswarapu, K. R. *J. Med. Chem.* **2003,** *46*, 3975.
17. Fulton, A. M.; Ma, X.; Kundu, N. *Cancer Res.* **2006,** *66*, 9794.
18. Jain, S.; Chakraborty, G.; Raja, R.; Kale, S.; Kundu, G. C. *Cancer Res.* **2008,** *68*, 7750.
19. Wang, D.; DuBois, R. N. *Nat. Rev. Cancer* **2010,** *10*, 181.
20. Praveen Rao, P.; Chen, Q.-H.; Knaus, E. E. *J. Med. Chem.* **2006,** *49*, 1668.
21. El Miedany, Y.; Youssef, S.; Ahmed, I.; El Gaafary, M. *Am. J. Gastroenterol* **2006,** *101*, 311.
22. Magda, A.-A.; Abdel-Aziz, N. I.; Alaa, A.-M.; El-Azab, A. S.; Asiri, Y. A.; ElTahir, K. E. *Biorg. Med. Chem.* **2011,** *19*, 3416.
23. Mozziconacci, J.-C.; Arnoult, E.; Bernard, P.; Do, Q. T.; Marot, C.; Morin-Allory, L. *J. Med. Chem.* **2005,** *48*, 1055.
24. Norouzi, M.; Norouzi, S.; Amini, M.; Amanzadeh, A.; Irian, S.; Salimi, M. *J. Cell. Biochem.* **2015,** *116*, 81.
25. Winfield, L. L.; Payton-Stewart, F. *Future Med. Chem.* **2012,** *4*, 361.
26. Mehrparvar, S.; Balalaie, S.; Rabbanizadeh, M.; Rominger, F.; Ghabraie, E. *Org. Biomol. Chem.* **2014,** *12*, 5757.
27. Musa, M. A.; Cooperwood, J. S.; Khan, M. O. F. *Curr. Med. Chem.* **2008,** *15*, 2664.
28. Piazzi, L.; Cavalli, A.; Colizzi, F.; Belluti, F.; Bartolini, M.; Mancini, F.; Recanatini, M.; Andrisano, V.; Rampa, A. *Bioorg. Med. Chem. Lett.* **2008,** *18*, 423.
29. Romeiro, N. C.; Aguirre, G.; Hernández, P.; González, M.; Cerecetto, H.; Aldana, I.; Pérez-Silanes, S.; Monge, A.; Barreiro, E. J.; Lima, L. M. *Biorg. Med. Chem.* **2009,** *17*, 641.

Figure Captions

Table 1. Chemical structure of compounds **7a-7t**.

Table 2. Inhibition of cell proliferation against HeLa, HepG2, F10, A549, 293T, L02 cells by target compounds (**7a-7t**)

Table 3. Inhibition activities of compounds (**7a-7t**) against COX-1/COX-2

Figure 1. Selective COX-2 inhibitors

Figure 2. Annexin V-FITC/PI dual-immuno-fluorescence staining after treatment with different concentrations of **7t** for different times revealed significantly increased number of apoptotic cells. (A) Compound **7t** induced apoptosis in HeLa cells with the density of 0, 1, 2, 4, 8 μM for 24 h were collected and processed for analysis. (B) Cells treated with 3 μM **7t** for different times (0, 12, 24, and 36 h) was collected and analyzed. The percentage of cells in each part was indicated. Images are representative of three independent experiments. Data are mean ±S.E.M. of three independent experiments (n=3). $^{*}P < 0.05$, $^{**}P < 0.01$.

Figure 3. Compound **7t** caused dose-dependent decrease of HeLa cell attachment. (A) Influence of **7t** on HeLa cell adhesion. (B) Influence of **Celecoxib** on HeLa cell adhesion. Data shown are the mean ±S.E.M. of three independent experiments (n=3). $^{*}P < 0.05$, $^{**}P < 0.01$.

Figure 4. Compound **7t** significantly inhibits HeLa cells migration and invasion. (A) The images (×100) of cells that migrated outside of transwell insert membrane in transwell migration assay. (B) The images (×100) of cells that invaded through the matrigel to outside of transwell insert membrane in transwell invasion assay. The number of migrated and invaded cells was counted in 16 random fields per chamber of three independent experiments (n=3). $^{*}P < 0.05$, $^{**}P < 0.01$.

Figure 5. The effects of **7t** (0.1 μM), **Celecoxib** (0.1 μM), LPS (0.1 μg/ml) on PGE_2 secretion in HeLa cells. Data shown are the mean ±S.E.M. of three independent experiments (n=3). $^{*}P < 0.05$.

Figure 6. The effects of PGE_2 (1 μM), **7t** (2μM) and **7t** (2 μM)+PGE_2 (1 μM) on HeLa cell proliferation, adhesion, apoptosis, migration, and invasion. (A) The effects of PGE2, **7t** and **7t**+PGE2 on cell proliferation were determined using MTT assay. (B) The effects of PGE_2, **7t** and **7t** +PGE_2 on cell adhesion. (C) The effects of PGE_2, **7t** (3 μM) and **7t** (3 μM) +PGE_2 on cell apoptosis. (D) The effects of PGE_2, **7t** and **7t** +PGE_2 on cell migration. (E) The effects of PGE_2, **7t** and **7t** +PGE_2 on cell invasion. Data shown are the mean ±S.E.M. of three independent experiments.

Figure 7. The histogram about CDOCKER_INTERACTION_ENERGY (-kcal/mol) of compounds (**7a-7t**) and **Celecoxib** for COX-2.

Figure 8. Molecular docking analysis of compound **7t** and **Celecoxib**, showing **7t** owned remarkable binding mode in COX-2. (A) Molecular docking 2D modeling of compound **7t** with COX-2: for clarity, only interacting residues are displayed. Three amino acids, **GLN203**, **HIS207**, **ASN382** was significant in the binding of ligand and formed four hydrogen bonds, two Pi bonds and a Sigma-Pi bond (B) Molecular docking 2D modeling of **Celecoxib** with COX-2: Three amino acids **HIS207, HIS386, TRP387** in enzyme formed two Pi bonds, a Sigma-Pi bonds and two hydrogen bonds with **Celecoxib**.

Figure 9. Molecular docking 3D modeling of compound **7t** with the COX-2 binding site: for clarity, only interacting residues are displayed.

Scheme 1[a].

Coumarin sulfonamides derivatives as potent and selective COX-2 inhibitors with efficacy in suppressing cancer proliferation and metastasis

Xiao-Yuan Lu[†], Zhong-Chang Wang[†]*, Shen-Zhen Ren, Fa-Qian Shen, Ruo-Jun Man, Hai-Liang Zhu*

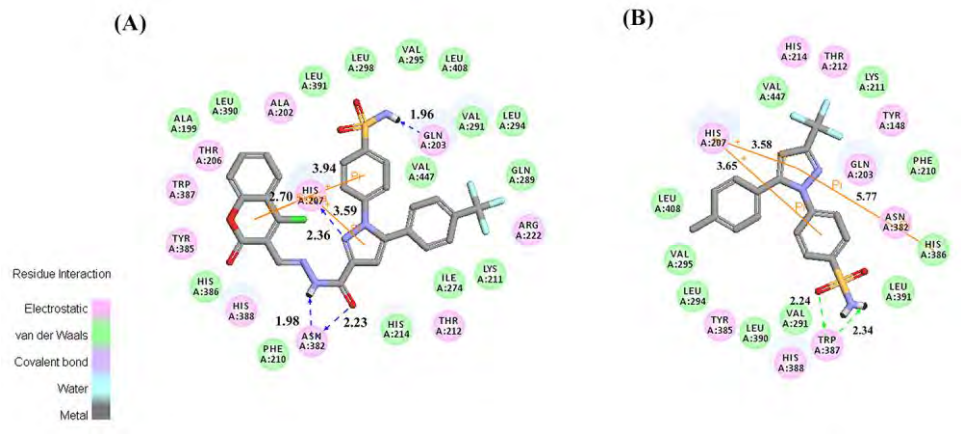

Novel Coumarin sulfonamides derivatives have been synthesized. Among them, compound **7t** showed most powerful selective inhibitory and antiproliferative activity. **7t** could effectively causing HeLa cells apoptosis in a dose and time-dependent manner and significantly suppress cancer cell adhesion, migration and invasion.